ADVANCES IN ATMOSPHERIC SCIENCES, VOL. 25, NO. 4, 2008, 641–654

Coupled Model Simulations of Climate Changes in the 20th Century and Beyond

YU Yongqiang*[1] (俞永强), ZHI Hai[1,2] (智 海), WANG Bin[1] (王 斌), WAN Hui[1] (万 慧), LI Chao[1] (李 超), LIU Hailong[1] (刘海龙), LI Wei[1] (李 薇), ZHENG Weipeng[1] (郑伟鹏), and ZHOU Tianjun[1] (周天军)

[1]*State Key Laboratory of Numerical Modeling for Atmospheric Sciences and Geophysical Fluid Dynamics (LASG), Institute of Atmospheric Physics (IAP), Chinese Academy of Sciences, Beijing* 100029

[2]*Nanjing Information and Technology University, Nanjing* 210044

(Received 30 April 2007; revised 18 January 2008)

ABSTRACT

Several scenario experiments of the IPCC 4th Assessment Report (AR4) are performed by version g1.0 of a Flexible coupled Ocean-Atmosphere-Land System Model (FGOALS) developed at the Institute of Atmospheric Physics, Chinese Academy of Sciences (IAP/CAS), including the "Climate of the 20th century experiment", "CO_2 1% increase per year to doubling experiment" and two separate IPCC greenhouse gases emission scenarios A1B and B1 experiments. To distinguish between the different impacts of natural variations and human activities on the climate change, three-member ensemble runs are performed for each scenario experiment. The coupled model simulations show: (1) from 1900 to 2000, the global mean temperature increases about 0.5°C and the major increase occurs during the later half of the 20th century, which is in consistent with the observations that highlights the coupled model's ability to reproduce the climate changes since the industrial revolution; (2) the global mean surface air temperature increases about 1.6°C in the CO_2 doubling experiment and 1.5°C and 2.4°C in the A1B and B1 scenarios, respectively. The global warming is indicated by not only the changes of the surface temperature and precipitation but also the temperature increase in the deep ocean. The thermal expansion of the sea water would induce the rise of the global mean sea level. Both the control run and the 20th century climate change run are carried out again with version g1.1 of FGOALS, in which the cold biases in the high latitudes were removed. They are then compared with those from version g1.0 of FGOALS in order to distinguish the effect of the model biases on the simulation of global warming.

Key words: greenhouse effect, coupled GCM, human activity

DOI: 10.1007/s00376-008-0641-0

1. Introduction

During the past century, the observed global mean surface air temperature shows a warming trend about 0.7°C±0.2°C. The 1990s may be the warmest decade of the instrumental records since 1861 and 1998 ranks as the warmest year. Radiosonde records show that the temperature of the troposphere below 8 km becomes warmer and warmer since the 1950s, about 0.1°C increase per decade. The global warming is indicated by the temperature changes, the changes of atmospheric and oceanic circulations and many other climate factors (IPCC, 2001). Since the global warming has a direct impact on human societies, it has become an important issue with scientists, the public and governments all over the world.

The climate changes may result from either the internal variability of the climate system or external forcing. Complicated feedbacks may exist among several other factors, while climate changes on various time scales would also compete and affect each other. The external forcing includes the solar insolation, volcanic eruptions, green house gas (GHG) and aerosol emissions induced by human activities, etc. Since the industrial revolution, the atmospheric GHG concentrations show an obvious increase. Taking the CO_2 for

*Corresponding author: YU Yongqiang, yyq@lasg.iap.ac.cn

example, the concentration remained about 280 ppm for a long time before 1850 but increased rapidly to 379 ppm by 2006. The analysis of the ice core records show that the present day CO_2 concentration may be the highest of the past 420 000 years (Petit et al., 1999). The concentrations of other GHG show a similar increase. From the qualitative physical aspect, the large increase of GHG concentrations can lead to the increase of the global surface air temperature. Meanwhile the ice core data indicate that the temperature changes have a positive correlation with the CO_2 concentration. But in terms of present studies, we can not easily come to a conclusion that the global warming over the past century is the result of an enhanced greenhouse effect. The increase of aerosol emissions or the cloud amount changes may reflect more solar insolation which offset the warming induced by GHG increase. It wasn't until the IPCC 3rd assessment report that the scientists came to a consensus that based on the latest evidence and the uncertainties, the observed warming of the past 50 years is mainly due to the increase of the GHG concentrations induced by human activities. However, the climate changes and the causes are very complicated and need more analysis (IPCC, 2001).

Because of the complicated processes of climate system, it is difficult to study the future climate change by using extrapolation, statistical methods or other experimental technologies. A feasible alternative is to study the climate system with numerical models because the climate model is a physical mathematic expression of the highly complicated nonlinear climate system. Corresponding to each component of climate system, the climate system model has relevant model components like atmospheric models, land surface models, ocean models, sea ice models, etc. During the past 30 years, the climate system model has experienced everything from individual model development to the whole coupled system model, of which both the atmosphere and ocean models are key components. With the continuous evaluation and improvement, the state-of-the-art coupled GCMs can provide credible simulations of sub-continental scale and seasonal to decadal time scale climate changes. The broad consistencies between model simulations and observations cause the coupled model to become an effective tool in studying the future climate changes quantitatively and also highlight its unique effect in the attribution of past global warming.

Since the pioneering work of Manabe and Wetherald (1975), many studies focus on the impacts of human activities on climate change by using climate models of different complication levels. Obviously, a better representation of past climate changes would increase the reliability of model simulations of future climate. Meanwhile, the climate model is a very convenient tool to study the causes of past climate changes. The simulations of 20th century climate changes have become an important issue. Many state-of-the-art coupled models can reproduce the global warming trend in the past century. Some model results show that the model can not reproduce the large warming of the past several decades when considering only the natural external forcing factors such as solar insolation changes, volcanic activities and the inertial interaction of the climate system. But considering both the impacts of natural factors and human activities, the coupled model simulates similar changes as in the observations. Therefore, the coupled model studies provide important scientific evidence for the basic conclusion of the IPCC 3rd assessment report that the observed warming of past 50 years is mainly due to the GHG concentration increase induced by human activities.

The GHG emission continues and the global warming tends to be more serious, therefore, how the global climate will change in the 21st century now becomes a very hot topic. To predict the future climate changes, we should first determine the possible GHG emission schemes. Six future GHG emission indicative scenarios and the relevant main GHG concentrations are provided in the IPCC 3rd assessment report (IPCC, 2001). For example, the CO_2 concentrations of the year 2100 will range from 540 ppm to 970 ppm. When considering the uncertainties of the Earth's biogeochemical cycle feedbacks, the range will expand to between 490 ppm and 1260 ppm. Due to the fact that the coupled model simulations consume huge computational resources, we cannot perform all of the possible scenario experiments. The one feasible method is to focus on minority scenarios, tuning the parameters of the simple model with the global coupled model results and adjusting the results of the simple model to the coupled model mean climates, and then simulate the future climate changes by using the adjusted simple model.

2. Model and experiment descriptions

2.1 *Coupled model description*

The coupled model FGOALS_g1.0 (Flexible Global Ocean-Atmosphere-Land System Model, Version g1.0) is used in this study. This model is the latest coupled climate system model developed at State Key Laboratory of Numerical Modeling for Atmospheric Sciences and Geophysical Fluid Dynamics (LASG), Institute of Atmospheric Physics (IAP), China Academy of Science (CAS). Four component models including atmo-

sphere, ocean, land surface and sea ice components are coupled through the NCAR coupler version 5 which computes and exchanges the heat flux, momentum and fresh water flux among models without any flux correction or adjustment. The ocean component model is a modified version of LICOM1.0 (Liu et al., 2004a,b). The major changes are: the model domain extends from 65°N to the North Pole and the horizontal resolution is reduced to $1° \times 1°$ due to the limited computational resource. The modified ocean model shows little differences from the original one but with a faster computational speed. The atmospheric component is GAMIL1.0, developed by introducing the physical processes of CAM2 into a new grid atmospheric dynamical framework (Wang et al., 2004). The horizontal resolution of GAMIL1.0 is about $2.8° \times 2.8°$ and the model simulations show a broad, correct pattern as in the observations. A thermal-dynamical sea ice component model is coupled to FGOALS_g1.0. This sea ice model has 5 levels in the vertical direction; its dynamical processes are based on the elastic-plastic rheology theory while the thermal processes are described by an energy conserved method (Bitz and Lipscomb, 1999). Since the coupler requests that the ocean and sea ice model have the same grids, the horizontal resolution of the sea ice model is modified to be the same as LICOM, as well as the sea-land distribution. For more detailed descriptions of the coupled model please refer to the work of Yu et al. (2002), Yu and Liu (2004), and Yu et al. (2007).

Recent diagnosis indicates that the coupled GCM FGOALS_g1.0 suffers from strong cold biases in high latitudes, e.g., there is a cooling trend in the control run, and the model overestimated sea ice extension in both the Northern and Southern Hemispheres (not shown here). Thus, the updated version g1.1 of FGOALS is developed by modifying the high latitude zonal filtering scheme and employing mass conservation rather than volume conservation in freshwater exchange (Yu et al., 2007) which causes the cold biases in high latitudes to be eliminated.

2.2 *Numerical experiment designs*

The following experiments are performed by the coupled climate model FGOALS_g1.0 according to the requirements of the IPCC AR4.

(1) Pre-industrial control experiment:

The concentrations of GHGs and sulfate aerosols and the solar constant are fixed to the pre-industrial value. The model has been integrated for 350 years in the experiment.

(2) CO_2 1% increase per year to doubling experiment:

Except for the CO_2 concentration, other external forcings are the same as the pre-industrial run. The CO_2 concentration increases 1% per year from 280 ppm and doubles in 70 years. After that the coupled model continues the integration for another 150 years with the CO_2 concentration fixed to the doubled value of 560 ppm. Therefore, the total length of this run extends to 220 years. To eliminate the impacts of the initial value, three ensemble runs are performed with different initial values. The three initial fields are taken from the values from January 1st of the model year 1, 6 and 10 of the pre-industrial control run, respectively.

(3) 20th century climate change experiment:

The objective of this experiment is to test the coupled model's ability in reproducing the climate changes of the 20th century forced by the actual external forcing of the past 150 years. The actual changes of three external radiation factors from 1850 to 2000 are introduced in the model, including all the GHG and sulfate aerosol concentrations and the solar constant. Three ensemble runs are performed as in the CO_2 doubling experiment.

(4) Committed Climate Change experiment:

This experiment starts on 1 January 2001 of the 20th century climate change experiment but fixes the three external radiation forcing to the values of the year 2000 and continues the model integration for 100 years. This experiment is to test the climate system's lagging response to the external forcing, because when giving the fixed radiation forcing the climate model needs a period of time to reach equilibrium. The lagging time in the coupled model is mainly determined by the deep ocean's response to the global warming. The adjustment of the deep ocean is accomplished by the thermohaline circulation, therefore the lagged time scale of the climate system to the external radiation forcing ranges from centuries to millennia. Such an experiment is seldom performed in the early climate change simulations; the CLIVAR/WGCM workshop highly suggests all the modeling groups should perform the committed climate change experiment based on the 20th century climate change and other different emission scenario experiments for the IPCC AR4. People have realized that the present day climate change is affected by the total amount of past GHG emissions and the GHG being released into the atmosphere at the present time may affect several centuries into the future. Therefore, the committed climate change experiment is of great importance to the comprehensive understanding of the GHGs effect on the climate change.

(5) IPCC A1B scenario experiment:

This experiment starts on 1 January 2001 of the 20th century climate change experiment and contin-

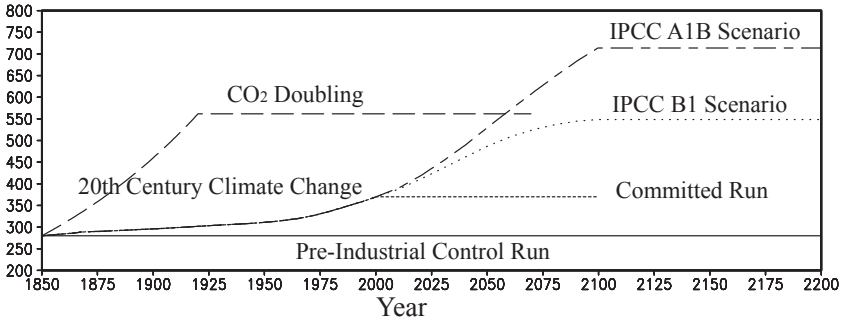

Fig. 1. The CO_2 concentration change of each IPCC AR4 experiments.

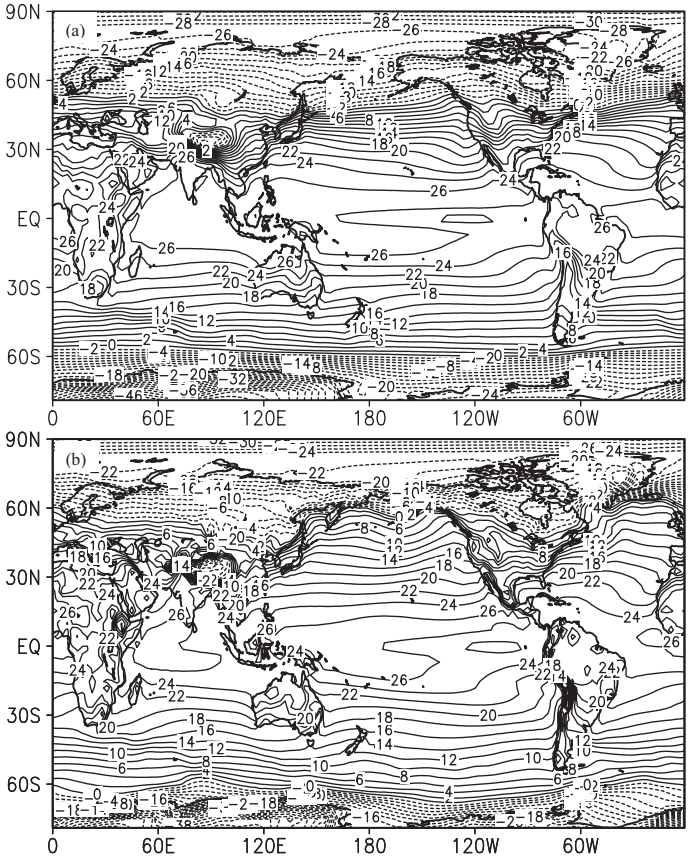

Fig. 2. Climatological mean surface air temperature from 20th century climate change experiment by (a) FGOALS_g1.0 and (b) g1.1. (unit: °C)

ues the model integration for 200 years so that the period of this experiment are from year 2000 to 2200. The GHG and sulfate aerosol concentrations are compliant to the requirement of the IPCC A1B emission scenario design between year 2000 and 2100. Then the GHG and sulfate aerosol concentrations are fixed to the value of year 2100 in the following 100 years in order to test the climate system's lagged response features of this scenario.

(6) IPCC B1 scenario experiment:

The start point, integration length, and the objective of this scenario are the same as the IPCC A1B experiment described above but with a different IPCC B1 GHG and sulfate aerosol emission design in the first 100 years.

The CO_2 concentration changes from all the above experiments are displayed in Fig. 1. All numerical experiments listed in Fig. 1 are carried out with the

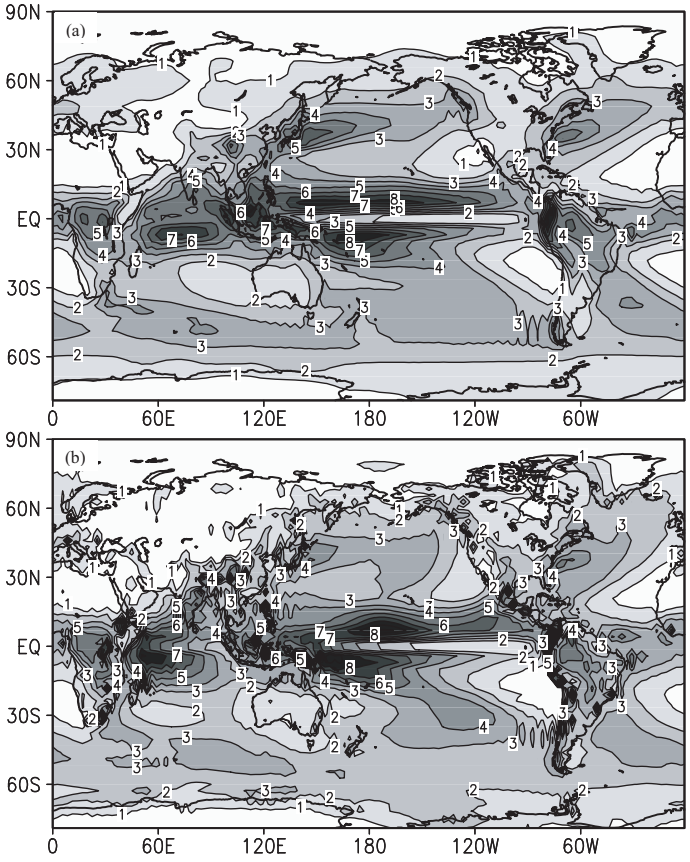

Fig. 3. Same as Fig. 2 except for precipitation. (Units: mm d^{-1})

IAP FGOALS_g1.0, and these simulations are submitted to the IPCC AR4 model data archive. In addition, both the industrial control run and the 20th century climate change run are carried out with FGOALS_g1.1 again and compared with those with FGOALS_g1.0 in order to discuss the uncertainty in the global warming simulation.

3. Surface air temperature and precipitation changes

Both versions of IAP coupled GCMs reproduce the observed large-scale pattern of climatological mean surface air temperature in the 20th century climate change experiments, but g1.0 shows a strong cold bias in the high latitudes (Fig. 2). The most striking error by g1.0 is characterized by much cooler temperatures in high latitudes, especially the simulated surface air temperature, which is about 10°C colder than the observed near Ice Island in the North Atlantic (Fig. 2a). As the simulated sea ice extension is reduced by about 40% in the version g1.1 (not shown here), the cold biases in the high latitudes are also reduced significantly (Fig. 2b), although there is about a 1°C –2°C cooling in the North Atlantic. In the tropical Pacific, the westward penetration of the cold tongue and warm bias off Peru can be found in both simulations, and many studies have suggested that it is a common tropical bias that existed in almost all of the coupled GCMs without flux correction and that it may be associated with radiation scheme, stratus cloud and the convective parameterization scheme etc. (Li et al., 2004; Dai et al., 2005). It is worth noting that the simulation of the western Pacific warm pool is much improved in version g1.1 than g1.0 because a new advection scheme is introduced in version g1.1 (Xiao, 2006).

Figure 3 shows simulated climatological mean precipitation by both versions from the 20th century climate change experiment; both models can simulate many of the major regional characteristics of the precipitation field, e.g., the structure of tropical precipitation from the two models is similar to the observation in the major convergence zones and also over the tropical rain forests. Also, strong rainfall belts along the storm track are well reproduced in the North Atlantic and North Pacific. Both models, however, are also generally deficient in reproducing some of the details of the observed precipitation. There is a distinct

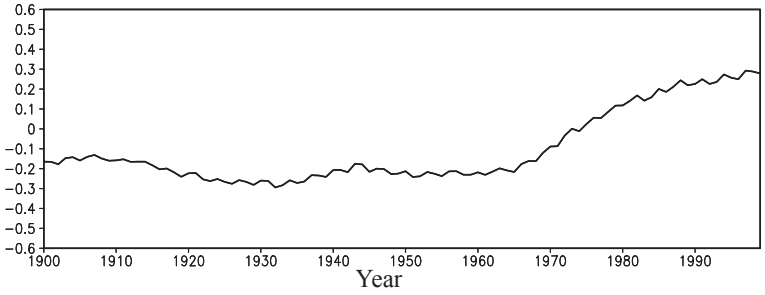

Fig. 4. The time series of the global mean surface temperature anomaly relative to the 30-year-mean between 1961 and 1990 from 20th century climate change experiment by FGOALS_g1.0. (units: °C)

tendency for the models to orient the South Pacific convergence zone parallel to latitudes and to extend it too far eastward, and it is the so-called "Double ITCZ" (Mechoso et al., 1995). It is strongly associated with an SST warm bias in the Southeastern Pacific.

The observed global mean surface temperature increased about 0.6°C±0.2°C over the whole 20th century (IPCC, 2001). Warming mainly occurred in two periods, one is around year 1940 and the other is after year 1975. Many studies suggest that the warming in the former half of 20th century is mainly due to the natural variations, probably related to the solar activities; while the warming in later half is mainly caused by the increase of GHG concentrations. Figure 4 displays the time series of the global mean surface temperature changes for each IPCC experiment described in section 2, the definition of deviation is the same as Fig. 2a. The coupled model reproduces the warming trend of 20th century in the 20th century climate change with a warming about 0.5°C which falls into the observed range. The model simulates a weak warming around 1940 and the other warming period starts from 1965 which leads the observations about 10 years. Overall, FGOALS_g1.0 succeeds in simulating the warming in the later half of 20th century, but shows a relatively weak ability to reproduce the warming around 1940 that needs further improvement. Similar deficiency also exists for most other 20th century climate change simulations, most of the coupled model that participated in the IPCC AR4 show diverse behaviors of simulating the warming around 1940 of which only a few models show a closer result to the observations, while nearly all the models reproduce the rapid warming of the past several decades (Zhou and Yu, 2006). Since the warming in past several decades is mainly caused by GHG concentrations increase, the simulations highlight the coupled models ability of simulating the warming caused by green house effect. The warming in the former half of 20th century may involve more complicated causes besides the increase of GHG, therefore by now we do not comprehensively understand the physical mechanisms involved and the coupled model lacks the ability to describe the mechanisms that causes the temperature changes.

The GHG emission of last century not only affected the climate of last century, but also will have impact on the future climate change for a long period. The 20th century committed climate change experiment shows that even if the GHG and aerosols concentrations are fixed to the value of year 2000, the global mean surface temperature will increase about 0.3°C (Fig. 5a). The simulations of A1B and B1 scenarios show similar warming trend. The global mean temperature of 2100 increases about 3.0°C and 2.0°C for A1B and B1 respectively when compared with the value averaged between 1961 and 1990. And from 2100 to 2200, although the GHG concentrations remain unchanged, the surface temperature continues to rise about 0.6°C and 0.4°C for A1B and B1 scenarios respectively. The temperature warming trend of above three experiments shows that the temperature increases rapidly in the first 100 years and slow down in the second 100 years due to the unchanged GHG concentrations. It is clear that the coupled system not yet reach an equilibrium state which further reveals the impacts of the atmospheric GHG on the climate change could last for more than 100 years.

Many observations show that the 20th century climate change is not only indicated by the global warming, but also some obvious changes of the atmospheric and oceanic circulations, especially the change in the precipitation. The land surface mean precipitation increased by 0.3% to 4% in the past 100 years, but the long term observations for the precipitation of most sea surface areas are lacking (Peterson and Vose, 1997; Chen et al., 2002). The coupled model experiments in this study show that the global (land surface) mean precipitation increases with the global warming. For example, the precipitation average for the land surface

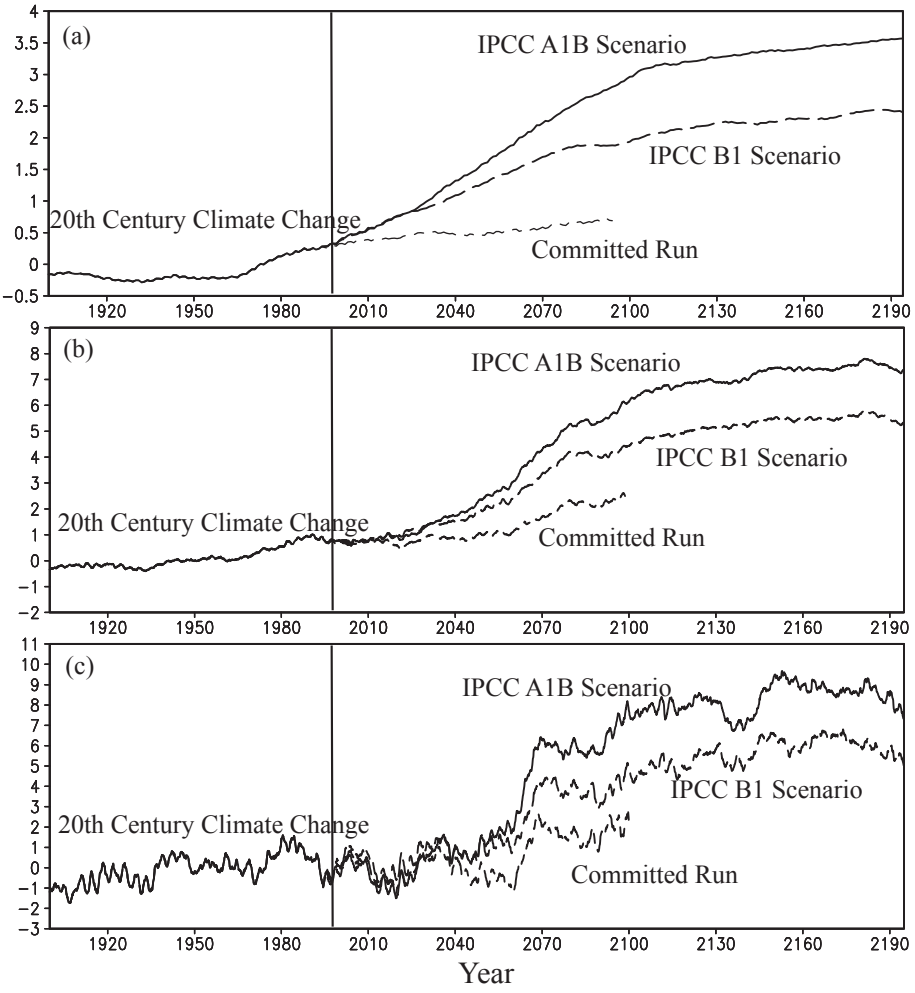

Fig. 5. The 10-year running mean time series for the 1990–2200 simulations of (a) global mean surface air temperature anomaly (deviation from the value averaged between 1961 and 1990, units: °C); (b) the global mean precipitation change in percentage (compared with the value averaged between 1961 and 1990, units: %); (c) the averaged mean precipitation change over land in percentage (compared with the value averaged between 1961 and 1990, units: %).

increased about 1.5% in the past 100 years, which is consistent with the observations. By 2200 the land surface precipitation increase about 8% and 6% for the A1B and B1 scenarios, respectively (Fig. 5c). The amplitude of global mean precipitation is relatively weaker, the model shows about a 1% increase in the past 100 years and 7.2% and 5.2% for the IPCC A1B and B1 scenarios (Fig. 5b).

Earlier numerical global warming simulations show that the warming caused by the GHGs is more significant in the mid-high latitude land area than that in the tropical regions and ocean areas (Manabe and Wetherald, 1975; Guo et al., 2001; Ma et al., 2004). The positive feedback of the high latitude ice and snow would enhance the warming while the large heat inertia of the ocean tends to weaken the warming of the ocean. Figures 4a and 4c show the simulated global surface temperature change around the year 2100 for IPCC A1B and B1 respectively, which are broadly in agreement with the early results. The largest warming simulated in this study is not located in the polar regions but is located over the oceans from about 50°S to 50°N that is different from most of other simulations. This may result from the coupled model's colder bias of the high latitudes in the control simulation. The simulated sea ice extension is much larger than the observations; the boundary of the sea ice and ocean is located at about 50°N/S while it is about 60°N/S in the observations. In the scenarios of A1B and B1, the sea ice decreases greatly and the region around 50°N/S which is originally covered by sea ice becomes an open sea surface, therefore the largest warming occurs where the sea ice

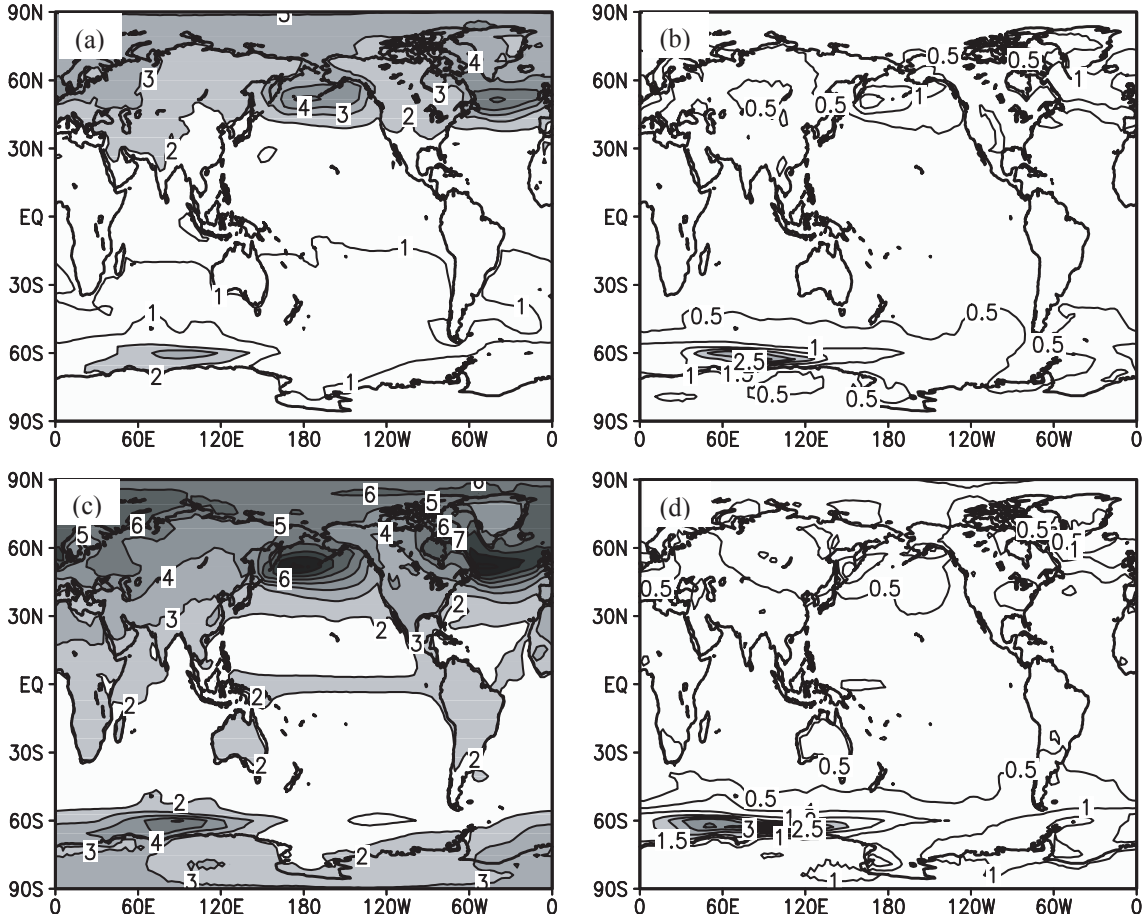

Fig. 6. (a) Change in surface air temperature averaged for 10 years from 2090 to 2100 relative to those averaged between 2000 and 2010 for B1 scenario; (b) change in surface air temperature averaged for 10 years from 2190 to 2200 relative to those averaged between 2100 and 2110 for B1 scenario; (c) the same as (a) but for A1B scenario; (d) the same as (b) but for A1B scenario.

decreases greatly through the positive feedback of ice and snow. Figures 4b and 4d display the simulated global surface temperature change in the second 100 years of A1B and B1 that indicates the model's lagging response to the total effect of all the radiation forcing.

More and more attention has been paid recently to regional climate change induced by human activity because of its direct impact on the environment and economy. The surface air temperature changes simulated by FGOALS_g1.0 for the IPCC A1B scenario in East Asia (10°–60°N, 60°–150°E) are shown in Fig. 7. The general warming pattern is similar to many previous studies (Chen et al., 1996; Guo et al., 2001; Gao et al., 2001; Jiang et al., 2004). For example, there is a larger warming in winter than in summer, and larger warming in the high latitudes than in low latitudes because of stronger ice(snow)-albedo-temperature positive feedback in the ice or snow covered regions. Although all greenhouse gases are fixed after year 2100, the significant warming is still found in East Asia, especially in winter. It is consistent with the temporal evolution of global mean surface air temperature (Fig. 6) because the ocean possesses huge heat inertia resulting in a delayed warming response to increasing GHGs. The simulation using the IPCC B1 scenario produces a very similar warming pattern but with weakened amplitude (not shown here).

4. The changes of deep ocean temperature and sea level

Due to the interactions among internal sub-systems of the climate system, the global warming caused by the greenhouse effect could reflect its impacts in each sub-system of the whole Earth's climate system. The observations and numerical studies indicate that both the upper and deep ocean are significantly becoming warmer in the past 100 years (Barnett et al., 2005). The 10-year running mean time series of volume-averaged temperature in the upper 300 m of the ocean

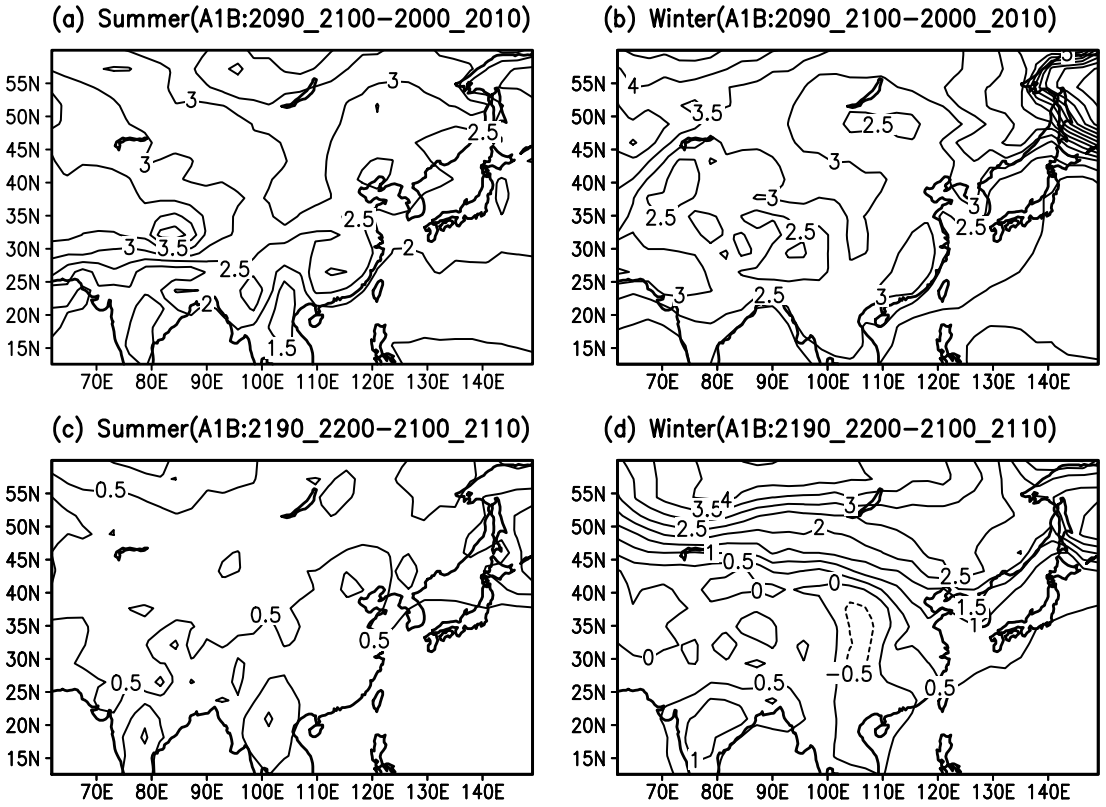

Fig. 7. (a) Change in summer (JJA) surface air temperature averaged for 10 years from 2090 to 2100 relative to those averaged between 2000 and 2010 for A1B scenario in East Asia; (b) change in winter (DJF) surface air temperature averaged for 10 years from 2090 to 2100 relative to those averaged between 2000 and 2010 for A1B scenario in East Asia; (c) the same as (a) but for the difference between 2190–2200 and 2100–2110; (d) the same as (c) but for the difference between 2190–2200 and 2100–2110.

is shown in Fig. 8. The amplitude of sea water temperature change in the upper 300 m is nearly equivalent to that of the global mean SST change (figure not shown), which indicates the amplitude of climate warming is basically uniform inside the thermocline. This may be related to the close interactions between the thermocline and the atmosphere and the response time scale of the thermocline to outer forcing ranges from interannual to decadal time scales. Therefore, the amplitude of thermocline change in response to centennial time scale climate change is equivalent to the sea surface.

The serious consequence of the global warming, especially the warming in the deep ocean, is the rise of the sea surface height because of the sea water thermal expansion. Nearly 50% of the world population lives in the areas within 500 km of the coastline, therefore, it is of great importance to project the sea level change in the future. Generally three mechanisms can cause the sea surface to rise: one is the movement of the lithosphere, the second is the thaw of the land ice sheet and the third is the sea water volume change caused by the density change. The observed sea surface rise is about 15–20 cm in the 20th century, of which about 1/3 to 1/2 is the contribution of the thermal expansion due to the warming of deep ocean (IPCC, 2001). Present coupled model in this study can not reproduce the changes of the lithosphere and ice sheets; therefore, we focus on the sea surface height caused by the sea water density change only. The time series of global mean sea surface level change estimated by the temperature and salinity change is shown in Fig. 9. It is similar to the observed estimate that the simulated global mean sea level rises about 4.5 cm due to heat expansion during the 20th century, and it keeps rising about 5 cm in the committed run in which all the radiative forcings are fixed at a constant as in year 2000. Therefore, the time scale of the response of the climate system to the external forcing should be much more than 100 years. For both the IPCC A1B and B1 scenarios, the coupled GCM projects the global sea level rise to be about 20 cm and 15 cm from 2000 to 2100, and about 20 cm and 12 cm from 2100 to 2200, respectively. The delayed response of the sea level and deep ocean temperature

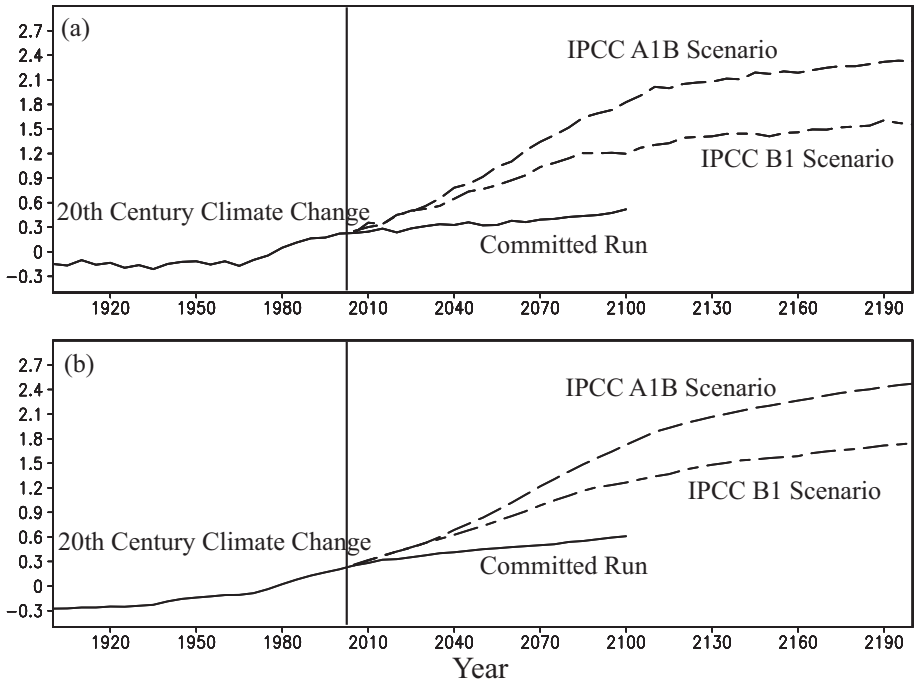

Fig. 8. 10-year running time series of (a) the global mean sea surface temperature anomaly, (b) of the global volume averaged sea temperature anomaly. (Unit: °C)

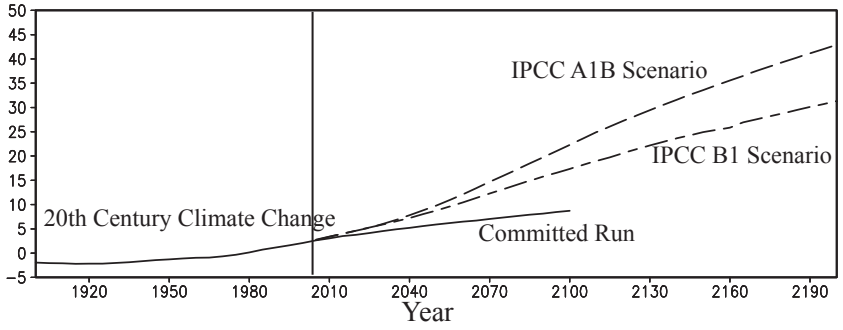

Fig. 9. The time series of the global mean sea level change of 1900–2200 (Units: cm).

actually implies that the emission of greenhouse gases has a persistent impact on the future climate change past hundreds of years.

5. Discussions

The coupled GCM FGOALS_g1.0 suffered from strong cold biases in the high latitudes. While these model biases are eliminated in FGOALS_g1.1, it is of great importance to compare simulations of global warming from two versions, g1.0 and g1.1, of FGOALS. The annual global mean surface air temperature of these two simulations are shown in Fig. 10, in which the models show nearly identical global warming trends around 0.5°C during the 20th century. It is worth noting that version g1.1 shows stronger interannual variability of temperature than g1.0, however both versions simulated similar variability in the low and middle latitudes, and it may be mainly attributed to stronger variability in the high latitudes in the latter (not shown).

Although versions g1.0 and g1.1 show very similar global warming trends in the 20th century climate experiment, the local linear trend simulated by g1.1 is significantly different from that simulated by g1.0 in the high latitude oceans (Fig. 11). For example, g1.0 shows stronger warming trends in the high latitudes, especially in the oceans, and weaker warming trends in the tropics compared to those shown by g1.1. Although cold biases of FGOALS_g1.0 amplified the re-

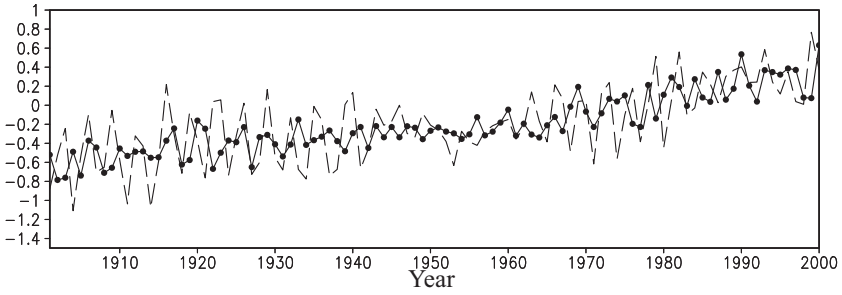

Fig. 10. 10-year moving averaged global mean surface air temperature anomaly relative to 1961–1990 mean temperature by FGOALS_g1.0 (dashed line) and g1.1 (solid line) during the 20th century (Units: °C).

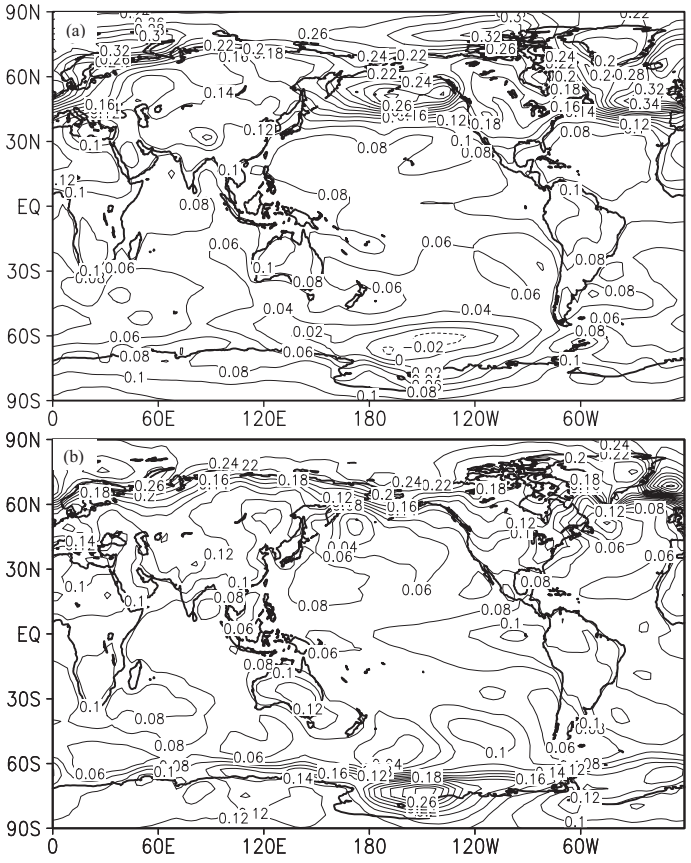

Fig. 11. The linear trend of surface air temperature from 1900 to 2000 by (a) FGOALS_g1.0 and (b) g1.1 [Units: °C (10 yr)$^{-1}$].

sponse of the model to the enhanced greenhouse effect in the high latitudes, which may be due to stronger positive ice-albedo-temperature feedback induced by overestimated sea ice extension in the model, it hardly impacts the climate sensitivity of the coupled models relative to the greenhouse effect. In fact, the climate sensitivity to increasing GHGs is mainly determined by the cloud feedback in the state-art-of coupled GCMs (Bony and Dufresne, 2005). Because both versions share the same cloud and radiation parameterization schemes, they show very similar responses in the global warming trends. Figure 12 shows temporal evolution of the net radiation anomaly at the top of the atmosphere relative to the 1961–1990 mean for FGOALS_g1.0 and g1.1 during the 20th century, in which both models simulate very similar linear increases in net energy input at the top of atmosphere. This is due to the fact that the same cloud-radiation

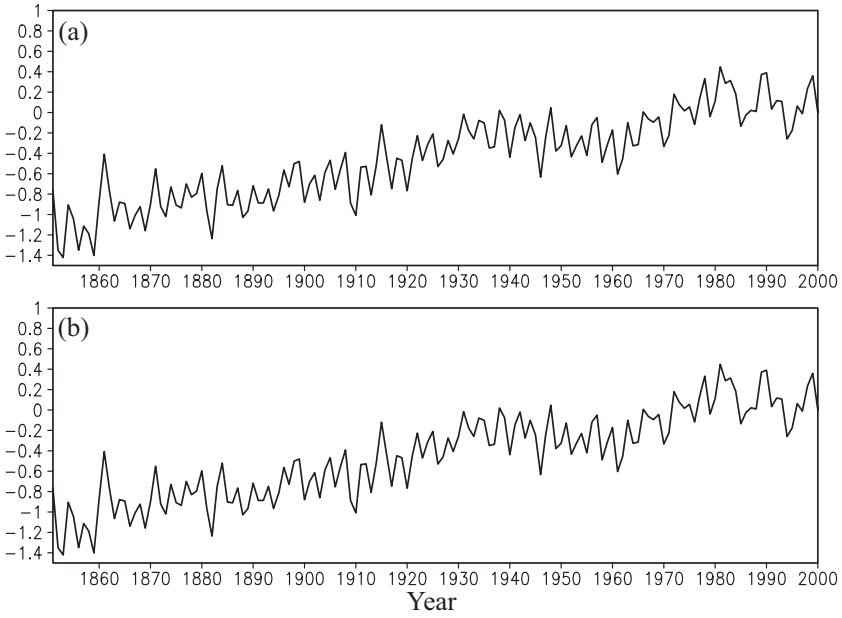

Fig. 12. 10-year moving mean net radiation anomaly relative to 1961–1990 mean averaged from 60°S–60°N by (a) FGOALS_g1.0 and (b) g1.1 during the 20th century. (Units: W m^{-2}).

feedback process is used.

In this study, a fully coupled GCM FGOALS_g1.0 was forced by the actual radiation forcing changes of the 20th century, induced by natural variation and human activities and the IPCC A1B and B1 GHG emission scenarios forcing of the 21st century. This is necessary in order to investigate the mechanism for the climate changes during the past 100 years and to project the future climate change in the next two centuries. The results show that the model can reproduce the global temperature, precipitation and sea surface height changes of the past 100 years forced by given GHG and aerosol concentrations and solar activities. Based on the simulation of the 20th century climate change, we continue the numerical simulations of future climate changes under the IPCC A1B and B1 scenarios. We also carried out the control run and the 20th century climate change run with an updated version g1.1 of FGOALS in order to explore the impacts of the cold biases on the simulation of global warming. The main conclusions are:

(1) The simulated global mean temperature increases about 0.5°C and the major warming occurs in the latter half of the 20th century. This is in broad agreement with the observations and indicates the coupled model can reproduce the climate change since the industrial evolution. The simulated global mean temperature increased about 1.5°C and 2.4°C for the IPCC A1B and B1 scenarios. The global mean precipitation increases as the temperature rises, and the simulated land surface precipitation increase about 1.5% in the past 100 years. This is consistent with the observations.

(2) Numerical experiment results show that the GHGs released into the atmosphere can affect not only the climate of present day but also the changes in future climate. For example, even if the GHG concentrations are fixed to the value of 2000, the global mean temperature will continue to increase about 0.5°C until 2100, precipitation will increase by about 1.5% and the sea surface height will rise 5 cm due to the thermal expansion of sea water. If in the next 100 years, the GHG emissions follow the situations of IPCC A1B and B1 scenarios, then until 2200, the global mean temperature will increase by about 2.4°C and 3.6°C, precipitation will increase about 5.2% and 7.2% and the sea surface will rise about 32 cm and 42 cm, respectively.

(3) The oceanic thermohaline circulation can transport the radiation heating forced by the GHGs into the deep ocean, thus increasing the temperature of the deeper sea water. Then, the thermal expansion of the ocean will raise the global mean sea surface height.

(4) Because the climate sensitivity of a coupled model is mainly attributed to the cloud-radiation interaction process, both simulations of the 20th century climate change, g1.0 and g1.1 of FGOALS, show almost identical climate sensitivity to increasing GHGs, and it implies that the local cooling trend hardly impacts the change of global mean surface air tempera-

ture. However, there are significant differences in the linear trends of surface air temperature in the high latitudes.

Compared with the observed climate changes in the 20th century, although the coupled model can reproduce the basic warming trend, the simulations of the warming around 1940 and the decadal variabilities are not yet satisfied. The deficiencies may be related to the uncertainties of the coupled model itself and the radiation forcing and the impact of initial fields. Actually, most of the coupled models that participated in the IPCC AR4 contain these kinds of deficiencies. It is even worse for the simulations of the future climate and until now people do not have a consensus of the GHG concentrations change in the next 100 years. Therefore, there will still be a need for work on coupled model development, improvement and evaluation for a long time to come.

Acknowledgements. We thank Mr. Wang Peng-Fei for the technology support of parallel computation. The computation of this study was carried on the LENOVO 6800 of the Computation Center of CAS and the IBM SP690 of the Scientific Computation and Information Center in IAP, CAS. The study is jointly supported by National Natural Science Foundation of China. (Grant Nos. 40675049, 40523001, and 40221503), National Basic Research Program of China "Ocean-Atmosphere Interaction over the Joining Area of Asia and Indian-Pacific Ocean (AIPO) and Its Impact on the Short-Term Climate Variation in China" (2006CB403605) and CAS Innovative Research International Partnership Project "The Climate System Model Development and Application Studies".

REFERENCES

Barnett, T. P., D. Pierce, K. AchutaRao, P. Gleckler, B. Santer, J. Gregory, and W. Washington, 2005: 18 Penetration of a warming signal in the World's oceans: human impacts. *Science*, **19**, doi:10.1126/science.1112418. 20

Bitz, C. M., and W. H. Lipscomb, 1999: An energy-conserving thermodynamic model of sea ice. *J. Geophys. Res.*, **104**, 15669–15677.

Bony, S., and J.-L. Dufresne, 2005: Marine boundary layer clouds at the heart of tropical cloud feedback uncertainties in climate models. *Geophys. Res. Lett.*, **32**, L20806, doi:10.1029/2005GL023851.

Chen, M., P. Xie, and J. E. Janowiak, 2002: Global land precipitation: A 50-yr monthly analysis based on gauge observations. *J. Hydrometeorol.*, **3**, 249–266.

Chen, Q. Y., Y. Q. Yu , Y. F. Guo, and X. H. Zhang, 1996: Climatic change in East Asia induced by greenhouse effect. *Climatic and Environmental Research*, **1**, 113–123. (in Chinese)

Dai, F. S., R. C. Yu, X. H. Zhang, Y. Q. Yu, and J. L. Li, 2005: Impacts of an improved low level cloud scheme on the Eastern Pacific ITCZ-Cold Tongue Complex. *Adv. Atmos. Sci.*, **22**, 559–574

Gao, X. J., Z. C. Zhao, Y. H. Ding, R. H. Huang, and F. Giorgi, 2001: Climate change due to greenhouse effects in China as simulated by a regional climate model. *Adv. Atmos. Sci.*, **18**(6), 1224–1230.

Guo, Y. F., Y. Q. Yu, X. Y. Liu, and X. H. Zhang, 2001: Simulation of climate change induced by CO_2 increasing for East Asia with IAP/LASG GOALS Model. *Adv. Atmos. Sci.*, **18**, 53–66.

IPCC, 2001: *Climate Change 2001: The Science of Climate Change. Contribution of Working Group 1 to Third Assessment Report of the Intergovernmental Panel on Climate Change*. Houghton et al., Eds., Cambridge University Press, Cambridge, United kingdom and New York, NY, USA, 881pp.

Jiang, D. B., H. J. Wang, and X. M. Lang, 2004: Multi-model ensemble prediction for climate change trend of China under SRES A2 Scenario. *Chinese Journal of Geophysics*, **47**(5), 878–886.

Li, J. L., X. H. Zhang, Y. Q. Yu, and F. S. Dai, 2004: Primary reasoning behind the double ITCZ phenomenon in a coupled ocean-atmosphere general circulation model. *Adv. Atmos. Sci.*, **21**, 857–867.

Liu, H. L., Y. Q. Yu, X. H. Zhang, and W. Li, 2004a: *LASG/IAP Climate System Ocean Model User Guide*. Science Press, Beijing, 128pp.

Liu, H. L., X. H. Zhang, W. Li, Y. Q. Yu, and R. C. Yu, 2004b: An eddy-permitting oceanic general circulation model and its preliminary evaluations. *Adv. Atmos. Sci.*, **21**, 675–690.

Ma, X. Y., Y. F. Guo, G. Y. Shi, and Y. Q. Yu, 2004: Numerical simulation of global temperature change over the 20th century with IAP/LASG GOALS Model. *Adv. Atmos. Sci.*, **21**, 227–235.

Manabe, S., and R. T. Wetherald, 1975: The effects of doubling the CO_2 concentration on the climate of a general circulation model. *J. Atmos. Sci.*, **32**, 3–15.

Mechoso, C. R., and Coauthors, 1995: The Seasonal cycle over the tropical Pacific in coupled ocean-atmosphere general circulation models. *Mon. Wea. Rev.*, **123**, 2825–2838.

Peterson, T. R., and R. S. Vose, 1997: An overview of the Global Historical Climatology Network Temperature Database. *Bull. Amer. Meteor. Soc.*, **78**, 2837–2848.

Petit, J. R., and Coauthors, 1999: Climate and atmospheric history of the past 420,000 years from the Vostok ice core, Antarctica. *Nature*, **399**, 429–436.

Xiao, C., 2006: Application of a shape-persevering advection scheme in an OGCM and Coupled GCM. M. S. thesis, Institute of Atmospheric Physics, Chinese Academy of Sciences, Beijing, China. (in Chinese)

Wang, B., H. Wan, Z. Z. Ji, X. H. Zhang, R. C. Yu, Y. Q. Yu, and H. L. Liu, 2004: Design of a new dynamical core for global atmospheric models based on some efficient numerical methods. *Science in China* (A), **47**(Suppl.), 4–21.

Yu, Y. Q., and X. Y. Liu, 2004: ENSO and Indian Dipole

Mode in Three Coupled GCMs. *Acta Oceanologica Sinica*, **23**, 581–595.

Yu, Y. Q., R. C. Yu, X. H. Zhang, and H. L. Liu, 2002: A flexible global coupled climate model. *Adv. Atmos. Sci.*, **19**, 169–190.

Yu, Y. Q., W. P. Zheng, H. L. Liu, and X. H. Zhang, 2007: The LASG Coupled Climate System Model FGCM-1.0. *Chinese Journal of Geophysics*, **50**, 1677–1687. (in Chinese)

Zhou, T. J., and R. C. Yu, 2006: 20th century Chinese temperature in coupled model simulations of IPCC AR4. *J. Climate*, **19**(22), 5843–5858.